A Novel Inductive Electromagnetic Energy Harvester For Condition Monitoring Sensors

N. M. Roscoe[1]*, M. D. Judd[1] and L. Fraser[2]
(1) University of Strathclyde, Glasgow, UK
(2) National Grid, Warwick, UK
*Email: nina.roscoe@eee.strath.ac.uk

***Abstract*— As the operation of electrical power networks becomes increasingly sophisticated, the role of condition monitoring is expanding. The burden of implementing additional condition monitoring will be eased if self-powered, fully autonomous sensors can be used to reduce installation and maintenance costs. Changing batteries is inconvenient and standard mains power is often not available where sensors are needed. Existing commercial inductive harvesters to power sensors must be fitted around high voltage transmission lines, which requires either a power outage or live line installation. In this paper, an alternative harvester is presented which can be installed at any location where there is sufficient magnetic field. Magnetic flux densities within a cable tunnel are considered, from which a suitable target is defined for the magnetic flux density range over which the harvester must provide power to the sensor. Optimisation of output power per unit volume limits cost and allows placement of sensors in locations with restricted space. Coil parameters to achieve high output power per unit volume are discussed and experimental results are presented that demonstrate effective energy harvesting. A coil design for a typical cable tunnel is proposed.**

Keywords – condition; monitoring; inductive; harvesting; energy; sensors; magnetic; coil

I. INTRODUCTION

The role of condition monitoring in the supply of electrical power is expanding, partly through the integration of distributed generation into the system and partly through the management of ageing assets. Effective condition monitoring can improve power supply reliability and lengthen asset life expectancy. However, providing energy to the condition monitoring sensors can be challenging due to the difficulty of changing batteries in a high voltage or extremely remote environment, together with the unavailability of mains power in many sensor locations. Several potential sources of available energy are identified near the condition monitoring locations in [1], including electromagnetic harvesting (capacitive and inductive), vibration and photovoltaic. All of these energy sources may have a role to play because no single solution will fit all condition monitoring applications. In this paper we propose a new form of inductive harvesting.

Inductive harvesting is currently utilised as an energy source for condition monitoring in applications where the harvesting device encloses the conductor [2], [3]. This arrangement, illustrated in Figure 1(a), is only practical where a sensor must be located on the HV point, and if the conductor is also of suitable diameter with adequate clearance around it. This method of "threaded" inductive harvesting is described in [4]. However, the majority of applications would require a harvester capable of operating in a magnetic field of much lower intensity, at a greater distance from the high voltage conductors. Such a device is a 'Free-standing harvester', as shown in Figure 1(b).

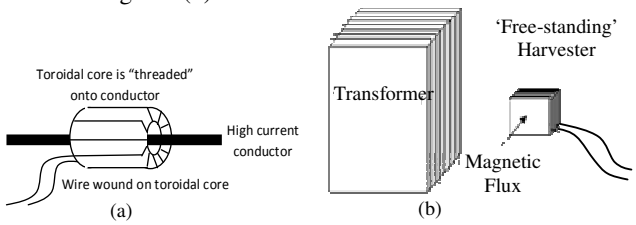

Figure 1 Inductive harvesting: (a) "Threaded" harvester enclosing a conductor, (b) "Free-standing" harvester sitting in magnetic field, e.g. near a transformer.

'Free-standing' harvesters have one significant disadvantage compared to 'threaded' harvesters: since the harvester does not enclose the source of the magnetic field, it is not possible to contain all of the magnetic flux inside a core. The consequent large 'air gap' dramatically reduces the output power per unit volume that can be delivered by a free-standing harvester for a given magnetic flux density. This disadvantage can be compensated for to some extent by the versatility of free-standing harvesters which do not need to enclose a conductor. For example, in a 'trough' style cable tunnel, as shown in Figure 2, it is not possible to enclose the conductor, there is no significant vibration, no sunlight, and very little electrostatic field (the cables are shielded). Hence a free-standing inductive harvester is the only self-powering option available.

II. MAGNETIC FLUX DENSITY

Variation of load current in cable tunnel conductors in the UK is typically between 50 A_{rms} and 2 kA_{rms}. To ensure optimum operation, the coil is to be designed to generate the desired output power at 50 A_{rms}, as this can be a persistent state. To proceed with design we must first ascertain the output power required by a typical wireless sensor, and the available magnetic flux density in the cable tunnel.

A. Wireless sensor power requirement

Using the analysis of sensor power consumption in [1], a low power sensor might require an average current of 80 µA at 5 V, a power requirement of 400 µW. The higher power

SunSPOT draws 200 µA when transmitting at the same duty cycle, which corresponds to 1 mW.

B. Magnetic Flux Density in Cable Tunnel

Double circuit cables are laid in a 'trough' style cable tunnel with the three phases in a 'trefoil' arrangement, see Figure 2. Unfortunately, while the resulting magnetic field cancellation makes them safer for use under residential areas, it also minimises the potential energy available for inductive harvesting.

The magnitude of the magnetic flux density as a function of radial distance from a current carrying conductor is given by

$$|\underline{B}| = \frac{\mu_o \mu_r I}{2\pi |\underline{R}|} \qquad (1)$$

Where μ_o is the permeability of free space ($4\pi 10^{-7}$), μ_r is the effective permeability of the core material, I is the current flowing in the wire (A), and R is the distance from the centre of the conductor (m).

Using (1), the magnitude of the contribution from each conductor in the trefoil can be calculated. In Figure 2, $\underline{R1}$, $\underline{R2}$ and $\underline{R3}$ are the vectors from the centre of each conductor to the centre of the harvester. The direction of the flux density is at 90° to the position vectors $\underline{R1}$, $\underline{R2}$ and $\underline{R3}$. To calculate the magnitude of the total magnetic field vector, the currents will be assumed to be balanced and in phase with their respective voltages.

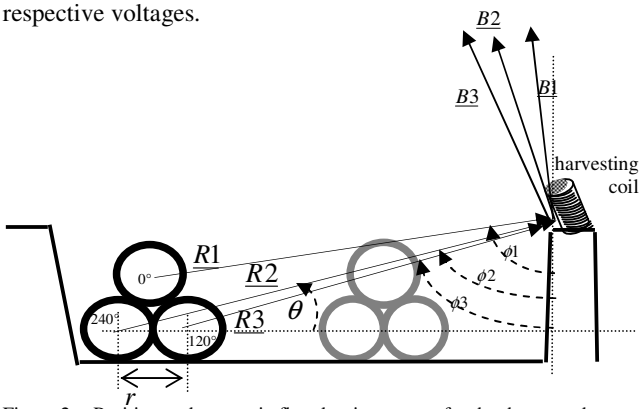

Figure 2 Position and magnetic flux density vectors for the three conductors in the left hand trefoil cable bundle, referred to the proposed harvester position, shown located on top of the side wall of the trough.

θ is the angle between the position vector $\underline{R2}$ and the horizontal. $\underline{R2}$ will be used a reference, from which the magnitudes of $\underline{R1}$ and $\underline{R3}$ can then be found:

$$|\underline{R1}| = \sqrt{\left(|\underline{R2}|\cos\theta - \frac{r}{2}\right)^2 + \left(|\underline{R2}|\sin\theta - r\sin\frac{\pi}{3}\right)^2} \qquad (2)$$

$$|\underline{R3}| = \sqrt{\left(|\underline{R2}|\cos\theta - r\right)^2 + \left(|\underline{R2}|\sin\theta\right)^2} \qquad (3)$$

The angles of the position vectors to the vertical are:

$$\phi 1 = \tan^{-1}\left[\frac{|\underline{R2}|\cos\theta - \frac{r}{2}}{|\underline{R2}|\sin\theta - r\sin\frac{\pi}{3}}\right] \qquad (4)$$

$$\phi 2 = \frac{\pi}{2} - \theta \qquad (5)$$

$$\phi 3 = \tan^{-1}\left[\frac{|\underline{R2}|\cos\theta - r}{|\underline{R2}|\sin\theta}\right] \qquad (6)$$

The magnitudes of the magnetic flux densities can then be found, using (1), (2) and (3):

$$|\underline{B1}| = \frac{\mu_o \mu_r I1}{2\pi\sqrt{\left(|\underline{R2}|\cos\theta - \frac{r}{2}\right)^2 + \left(|\underline{R2}|\sin\theta - r\sin\frac{\pi}{3}\right)^2}} \qquad (7)$$

$$|\underline{B2}| = \frac{\mu_o \mu_r I2}{2\pi|\underline{R2}|} \qquad (8)$$

$$|\underline{B3}| = \frac{\mu_o \mu_r I3}{2\pi\sqrt{\left(|\underline{R2}|\cos\theta - r\right)^2 + \left(|\underline{R2}|\sin\theta\right)^2}} \qquad (9)$$

where $\underline{I1}$, $\underline{I2}$ and $\underline{I3}$ are the currents in the conductors corresponding to $\underline{R1}$, $\underline{R2}$ and $\underline{R3}$ respectively. The phase of the current in each conductor is shown in Figure 2. $\underline{I1}$, $\underline{I2}$ and $\underline{I3}$ are all equal in amplitude and can be expressed:

$$I1 = I\sin\omega t \qquad (10)$$

$$I2 = I\sin\left(\omega t + \frac{4\pi}{3}\right) \qquad (11)$$

$$I3 = I\sin\left(\omega t + \frac{2\pi}{3}\right) \qquad (12)$$

The magnitude of the sum of magnetic flux density contributions from all three cables can then be found, by summing horizontal and vertical components.

$$Bx_{tot} = |\underline{B1}|\sin\left(\phi 1 + \frac{\pi}{2}\right) + |\underline{B2}|\sin\left(\phi 2 + \frac{\pi}{2}\right) + |\underline{B3}|\sin\left(\phi 3 + \frac{\pi}{2}\right) \qquad (13)$$

$$\Rightarrow Bx_{tot} = -|\underline{B1}|\cos\phi 1 - |\underline{B2}|\cos\phi 2 - |\underline{B3}|\cos\phi 3$$

$$By_{tot} = |\underline{B1}|\cos\left(\phi 1 + \frac{\pi}{2}\right) + |\underline{B2}|\cos\left(\phi 2 + \frac{\pi}{2}\right) + |\underline{B3}|\cos\left(\phi 3 + \frac{\pi}{2}\right) \qquad (14)$$

$$\Rightarrow By_{tot} = -|\underline{B1}|\sin\phi 1 - |\underline{B2}|\sin\phi 2 - |\underline{B3}|\sin\phi 3$$

$$B_{tot} = \sqrt{Bx_{tot}^{\ 2} + By_{tot}^{\ 2}} \qquad (15)$$

Representative cable tunnel dimensions provided by National Grid were $r = 118mm$, $|\underline{R}| = 744mm$ and $\theta = 0.55$ radians. Using these dimensions in equations (1) to (15), the total magnetic flux density for conductor currents of 50 A_{rms} was found to be 4.5 uT_{rms}.

III. EXPERIMENTAL SET-UP

Maxwell demonstrated that using three concentric coils it is possible to create an almost constant magnetic field in the space inside the coils [5]. If a is the radius of the centre coil, then the two outer coils must be separated from the centre one by a distance $\sqrt{3/7}a$, and the radius of each of the outer coils must be $\sqrt{4/7}a$. The ampere-turns of the outer two coils must be equal to 49/64 that of the inner coil. The Maxwell coil set used for these experiments had a centre coil of radius 760 mm.

Output voltage across the load on the output of the harvester coil was measured on an oscilloscope, from which output power was calculated.

IV. Optimum Coil Design

While the closed loop of magnetic flux from the conductors is only partially intersected by the core of a free-standing harvester, a core material with permeability greater than that of free space yields greater output power per unit volume than an air core. However, fringing effects mean that optimum geometry of the core is not immediately obvious. Hence experimental results were used to determine optimum coil geometry for coils with higher permeability cores.

Figure 3 shows the equivalent circuit of the coil in series with a resonant capacitor, C_S, and terminated by a matched load resistor to maximise output power. The resonant capacitor is similar to the compensating series capacitors in [6,7].

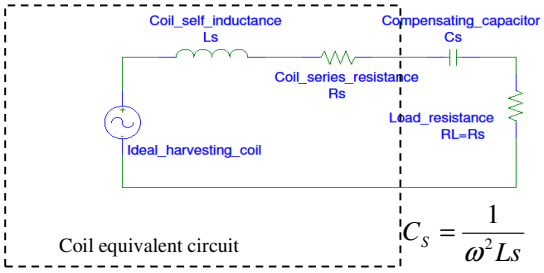

Figure 3 Equivalent circuit for coil with ideal matching impedance. Coil inductance is resonated out by series capacitor, Cs.

Open circuit voltage on an air-cored coil in the presence of flux density, $V_{o/c}$ (V_{rms}), is found from equation (16).

$$V_{o/c} = 2\pi fNAB \tag{16}$$

where N = number of turns on the coil, A = cross sectional area of the coil (m^2), B = Magnetic flux density (T_{rms}) and f = frequency of the magnetic field (Hz).

For a harvesting coil with compensating capacitor, the number of turns should be the maximum that can be practically fitted onto the core to deliver maximum output power.

When a core wholly contains the magnetic path, then (17) gives the open circuit coil voltage.

$$V_{o/c} = 2\pi f\mu_r NAB \tag{17}$$

where μ_r is the relative permeability of the core material. However, in the case of an inductive harvester, where the loops formed by the magnetic field lines only partially intersect the coil, we can define an 'effective' relative permeability as follows:

$$V_{o/c} = 2\pi f\mu_{eff} NAB \tag{18}$$

where $1 < \mu_{eff} < \mu_r$.

Inductance of a coil, L (H), with length to diameter ratio greater than 0.4 is given in [8]

$$L = \frac{\pi\mu r^2 N^2}{l + 0.9r} \tag{19}$$

where r is the radius of the coil (m), $\mu = \mu_0\mu_{eff}$ and $\mu_0 = 4\pi \times 10^{-7}\, H/m$ is the permeability of free space. Equation (19) can be rearranged to calculate μ_{eff} from measured inductance:

$$\mu_{eff} = \frac{L(l + 0.9r)}{\pi\mu_0 r^2 N^2} \tag{20}$$

Coil inductance was measured on a bridge, and the results used in (20) to calculate effective permeability.

Output voltage, V_{out} (V_{rms}), generated across load resistance in Figure 3, during application of an external magnetic field, is exactly half the open circuit coil voltage found in (18).

$$V_{out} = \frac{V_{o/c}}{2} = \pi f\mu_{eff} NAB \tag{21}$$

Effective core permeability can therefore also be calculated from measured induced voltage by rearranging (21):

$$\mu_{eff} = \frac{V_{out}}{\pi fNAB} \tag{22}$$

Output voltage, P_{out} (W), can be converted to output power using:

$$P_{out} = \frac{V_{out}^{\ 2}}{Rs} \tag{23}$$

Measurements were carried out in a uniform B-field generated by the Maxwell coils described previously. A range of coil geometries were measured, with four different core materials: laminated steel $\mu_r \approx 600 - 2000$ [9,10], cast iron $\mu_r \approx 200$ [10], ferrite 3C90 $\mu_r \approx 1720$ [11] and ferrite 3F4 $\mu_r \approx 840$ [11]. All measurements were made in a magnetic flux density of 700 uT_{rms}, and there were 1000 turns on each coil.

Figure 4 shows effective permeability as a function of coil length to diameter ratio, calculated using (20), and Figure 5 shows output power per unit volume as a function of coil length to diameter ratio. In Figure 5, output power was calculated from equation (23) using the output voltages measured in the Maxwell coils described above.

Values of effective core permeability were calculated using both (20) and (22). Comparisons between the two permeability values showed they were equal to within about ± 30 % for laminated steel and cast iron, and ± 7 % for 3F4 and 3C90 cores. This suggests that the fringing effects of magnetic flux density are similar whether the magnetic field is generated by a current in the coil itself, or whether the coil is placed in a uniform external magnetic field. Equation (21) therefore predicts coil output voltage generated in an external magnetic field using effective permeability calculated from measurements of coil self inductance. The performance of any coil used as an inductive harvester in a quasi-uniform field is simple to predict if the self inductance of the coil is known.

From Figure 5 it can be seen that the optimum shape for output power per unit volume is a long and thin solenoid, i.e. maximum coil length to diameter ratio.

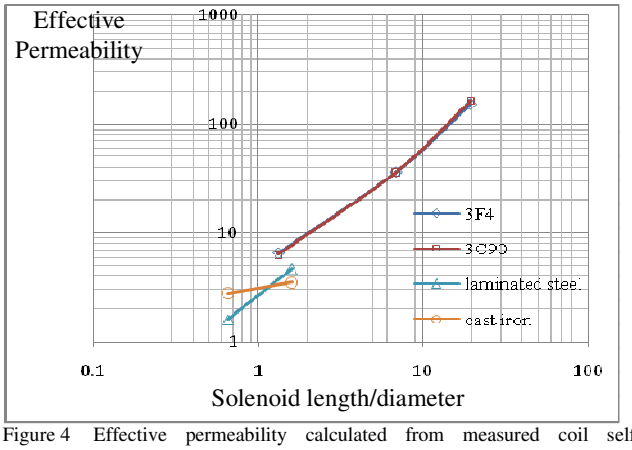

Figure 4 Effective permeability calculated from measured coil self inductance.

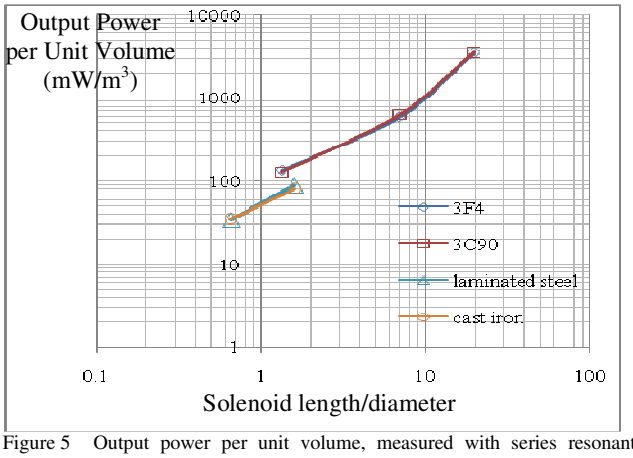

Figure 5 Output power per unit volume, measured with series resonant capacitance, into a matched load.

The material used for the core appears to have a comparatively small effect on output power per unit volume, leading to similar effective permeability values for different materials. Therefore, if the inherent permeabilities of the materials are all much higher than the effective permeability for the chosen geometry, then the material which is cheapest and easiest to work with should be chosen. Amongst the materials tested, this is therefore likely to be cast iron.

V. Cable Tunnel Harvester Size

Interpolations from the measured values of effective permeability in section IV have been used to estimate the coil size required to generate 1 mW of power for a (pessimistic) value of 4.5 uT_{rms} magnetic flux density using MathCAD. An empirical expression for effective permeability as a function of length to radius ratio was derived from the data presented in Figure 4:

$$\mu_{eff} = 4\left(\frac{l}{2r}\right)^{1.25} \qquad (24)$$

For the location of the harvester shown in Figure 2 a plot of coil length vs coil radius can be generated using (20), (21) and (23), as shown in Figure 6. It has been assumed that wire diameter is 0.22 mm, and that the practical maximum number of turns is about 500 for every 20 mm length.

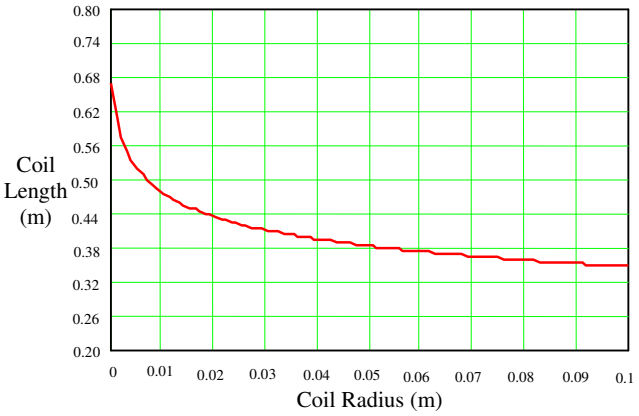

Figure 6 Coil geometry required to generate 1 mW in 4.5 uT_{rms} flux density for the location shown in Figure 2.

VI. Conclusions

A novel "free-standing" inductive harvester has been presented. Minimum magnetic flux density available for operation in a typical National Grid cable tunnel has been calculated to be 4.5 uT_{rms}. Optimum coil design has been investigated using a combination of theory and measurement, leading to a useful design model for the free-standing inductive harvester. A harvester coil of radius 0.012 m and length 0.6 m is proposed to deliver 1 mW for a "trough" style cable tunnel harvester .

VII. Acknowledgements

This research has been carried out within a project funded by National Grid (project reference 227819/FFR).

VIII. References

[1] M Zhu, P Baker, N M Roscoe, M D Judd and J Fitch, "Alternative Energy Sources for Autonomous Sensors in High Voltage Plants", Proc. 29th IEEE Electrical Insulation Conference (EIC 2009), (Montreal, Canada), June 2009.

[2] C&G – Overhead Transmission Line Monitoring (OTLM), Datasheet, www.c-g.si.

[3] http://www.oe.energy.gov/DocumentsandMedia/Low_Cost_Sensors_for_Real_Time_Monitoring_Fish.pdf, May 2010.

[4] Development of magnetic induction energy harvesting for condition monitoring Roscoe, N.M.; Judd, M.D.; Fitch, J.; Universities Power Engineering Conference (UPEC), 2009 Proceedings of the 44th International Publication Year: 2009

[5] Clerk-Maxwell, James (1873). *Treatise on Electricity and Magnetism*. Oxford: The Clarendon Press. ISBN 0-486-60636-8. Page 319.

[6] A. Esser and H.-C. Skudelny, "A new approach to power supplies for robots," *IEEE Trans. Ind. Applicat.*, vol. 27, pp. 872–875, Sept./Oct. 1991.

[7] G. A. Covic, G. Elliott, O. H. Stielau, R. M. Green, and J. T. Boys, "The design of a contact-less energy transfer system for a people mover system," in *Proc. Int. Conf. Power System Technology*, vol. 1, Dec. 2000, pp. 79–84.

[8] S. Ramo, J.R. Whinnery and T. Van Duzer, "Fields and Waves in Communications Electronics", John Wiley & Sons, 1984, ISBN 0-471-81103-3, p. 192.

[9] "Handbook of Electric Motors", Hamid A. Toliyat, G. B. Kliman, Marcel Dekker, Inc. 2004, ISBN 0-8247-4105-6, Page 201.

[10] "Engineering Science" by W. Bolton, Elsevier Newnes, 2006, ISBN 13: 978-0-7506-8083-7, Page 174.

[11] Ferroxcube company web-site www.ferroxcube.com, June 2010.